Pergamon

Int. J. Solids Structures Vol. 33, No. 13, pp. 1867–1889, 1996

0020-7683/96 $15.00 + .00

0020-7683(95)00138-7

A METHOD FOR THERMO-MECHANICAL ANALYSIS OF STEADY STATE DYNAMIC CRACK GROWTH

J. A. KALLIVAYALIL, C. Y. HUI and A. T. ZEHNDER
Department of Theoretical and Applied Mechanics Cornell University, Ithaca, NY 14853, U.S.A.

(*Received* 24 *January* 1995; *in revised form* 2 *June* 1995)

Abstract—Cracks propagating at high speeds in metals generate heat at their tips which cannot be conducted away in the very short time span of crack growth. The effect of heating on the crack tip stress fields and on dynamic fracture toughness is analyzed using a method based on the theory of generalized analytic functions. In this method all deviations from a linear elastic, homogeneous strain field are represented as fictitious body forces, allowing one to model inelastic and thermal effects. Numerical computations of the crack tip stress and strain fields are performed assuming steady-state, plane stress, mode-I dynamic crack growth with a fixed crack tip temperature field, but with temperature and strain rate sensitive mechanical properties. The relationship between dynamic stress intensity factor and crack velocity has been determined using competing ductile and brittle fracture criteria. A careful analysis of the trailing wake has been performed to study its effect on the crack tip stress field.

1. INTRODUCTION

When a crack grows through a metal that allows for some plastic deformation ahead of the crack tip, an increase in temperature will be induced in a region around the crack tip. The source of this temperature rise is the conversion of plastic work to heat. When the crack growth speed is fast relative to the "speed" of thermal conduction, determined by the material's thermal diffusivity, there is insufficient time for the heat generated to conduct away from the crack prior to fracture. Thus temperature builds up in the crack tip plastic zone. Because of the potential implications of the temperature rise at the crack tip on the dynamic fracture process, various attempts have been made to numerically simulate the temperature field at the crack tip. Rice and Levy (1969) esimated the temperature rise from the plastic dissipation using a Dugdale model. Weichert and Schönert (1974) assumed a uniform circular distribution and later a uniform rectangular distribution (1978) to simulate the temperature field. Kuang and Atluri (1985) used a moving mesh finite element analysis to simulate the temperature field due to a uniform rectangular distribution and also due to a singular $1/r$ type distribution. Krishnakumar *et al.* (1989) and Deng (1994) used the plastic dissipation from isothermal finite element calculations to estimate the temperature field at the crack tip. With the advent of high speed infrared detectors, Zehnder and Rosakis (1991), Rosakis *et al.* (1993) and Kallivayalil and Zehnder (1994) have demonstrated that reliable measurements of the crack tip temperature field can be made even when the crack speeds are of the order of 1000 m/s. In all cases the temperature rise is 300–500 C. This temperature rise is significant enough to affect the material properties and perhaps the mode of fracture itself. It is the intent of this paper to present a method for determining the effect of an imposed temperature field on the dynamic fracture process.

The problem of a steadily growing mode I crack in plane stress under small scale yielding conditions is considered here. A small strain, small displacement theory of continuum mechanics is assumed, thus an additive decomposition of strain into elastic and non-elastic parts is permissible, i.e.,

$$\underline{\varepsilon} = \underline{\varepsilon}^e + \underline{\varepsilon}^i = \tfrac{1}{2}(\nabla \mathbf{u} + \nabla \mathbf{u}^T). \tag{1}$$

In this work, the non-elastic strains will be treated as an incompatible strain, $\underline{\varepsilon}^i$, in an elastic body. The incompatible strains may be due to plastic deformation, $\underline{\varepsilon}^{pl}$, or thermal expansion, $\underline{\varepsilon}^{th}$,

$$\underline{\varepsilon}^i = \underline{\varepsilon}^{pl} + \underline{\varepsilon}^{th}, \quad \underline{\varepsilon}^{th} = \alpha I(T - T_o), \tag{2}$$

where T is the temperature and T_o is the reference temperature, α is the co-efficient of thermal expansion and I the identity tensor. The self stress caused by the incompatible strains, $\underline{\varepsilon}^i$, is determined by the method of fictitious body forces, first suggested by Eshelby (1957). A systematic method for calculating self stresses for static problems was developed by Wu and Hui (1986), and the method was further extended to solve steady state dynamic crack problems by Wu (1988). This formulation has the advantage that only the plastically deformed region at the crack tip needs to be discretized as opposed to finite element formulations where the elastic region surrounding the plastic region has to be discretized too. The formulation presented here provides the mathematical details for solving steady state dynamic fracture problems and is particularly suited for rate dependent materials as the steady state condition allows us to represent material derivatives in terms of derivatives in the direction of crack propagation in a crack tip co-ordinate system, i.e., in a co-ordinate frame (x, y) moving with the crack tip in the positive x direction,

$$\left.\frac{D}{Dt}\right|_{mat} = -v\frac{\partial}{\partial x} \tag{3}$$

where v is the crack tip velocity.

The effect of temperature on the dynamic fracture process is studied by imposing a temperature field at the crack tip. The maximum temperature imposed is representative of experimentally determined fields. The variation of the yield stress with temperature, the softening due to the drop in elastic modulus and the differential thermal expansion are explicitly included in our model. As the dynamic fracture process involves high strain rates, a constitutive law that reflects these rate effects, similar to that used by Freund and Hutchinson (1985) has been selected. The ductile to brittle transition is studied by considering competing crack growth criteria.

A careful analysis of the wake region behind the crack is also performed to determine its effect on the crack tip stress fields. In determining the effect of the incompatible strain in an elastic body, it is necessary to modify the boundary conditions of the original problem, by the imposing of tractions defined by $-\underline{\underline{C}} : \underline{\varepsilon}^i \cdot \mathbf{n}$, where $\mathbf{n}$, is the outward pointing normal in the region where the domain of the incompatible strain intersects the boundary of the body. In this work, these pseudo-tractions have been ignored and the implications of doing so are discussed.

2. PRELIMINARY RESULTS FROM COMPLEX CALCULUS

A complex function $f(z)$ is defined by

$$f(z) = f(x, y) = u(x, y) + iv(x, y), \tag{4}$$

where u and v are real valued functions. By $f(\bar{z})$ we mean

$$f(x, -y) = u(x, -y) + iv(x, -y). \tag{5}$$

Further we use $\tilde{f}(z)$ to denote $\overline{f(\bar{z})}$,

$$\tilde{f}(x, y) = u(x, -y) - iv(x, -y). \tag{6}$$

It should be noted that if f is analytic in a complex domain Ω, then so is $\tilde{f}$ in $\bar{\Omega}$, the domain conjugate to Ω. We define the following complex differential operators,

$$\partial_z = \tfrac{1}{2}\left(\frac{\partial}{\partial x} + i\frac{\partial}{\partial y}\right), \quad \partial_{\bar{z}} = \tfrac{1}{2}\left(\frac{\partial}{\partial x} - i\frac{\partial}{\partial y}\right). \tag{7}$$

Note that when the operator $\partial_{\bar{z}}$ acts on an analytic function it does result in its derivative. Some results that follow from the definition of the above operators are

$$\partial_z f = \overline{\partial_{\bar{z}} \tilde{f}}, \quad \partial_{\bar{z}} f = \overline{\partial_z \tilde{f}}. \tag{8}$$

It follows from the Cauchy–Reimann conditions for an analytic function f that,

$$\partial_{\bar{z}} f = 0, \quad \partial_z (fg) = f \partial_z g, \tag{9}$$

where g is any general function of a complex variable.

2.1. *Solution of a boundary value problem*

Consider a two dimensional vector function $\mathbf{f} = u\mathbf{i} + v\mathbf{j}$, with continuous partial derivatives, defined over a simply connected domain A with boundary ∂A, where **i**, **j** are the unit vectors in the Cartesian x and y directions. Green's formula is given by

$$\int_A \left(\frac{\partial v}{\partial x} - \frac{\partial u}{\partial y}\right) \mathrm{d}A = \oint_{\partial A} u\,\mathrm{d}x + v\,\mathrm{d}y. \tag{10}$$

Let $f \equiv u + iv$ then using Green's formula it can be verified that,

$$\int_A \partial_z f \,\mathrm{d}A = \frac{1}{2i}\oint_{\partial A} f\,\mathrm{d}z, \quad \int_A \partial_{\bar{z}} f\,\mathrm{d}A = -\frac{1}{2i}\oint_{\partial A} f\,\mathrm{d}\bar{z}, \tag{11}$$

where $\mathrm{d}A = \mathrm{d}x\,\mathrm{d}y$, $\mathrm{d}z = \mathrm{d}x + i\,\mathrm{d}y$, $\mathrm{d}\bar{z} = \mathrm{d}x - i\,\mathrm{d}y$. Consider the problem

$$\partial_z f = g(z), \quad z \in A \tag{12}$$

$$f = h(z), \quad z \in \partial A. \tag{13}$$

The solution to (12) is the sum of a particular solution and the homogeneous solution. The homogeneous solution corresponds to an analytic function whose value is specified on the boundary. For the domain A in Fig. 1, the solution was obtained by Vekua (1962) as

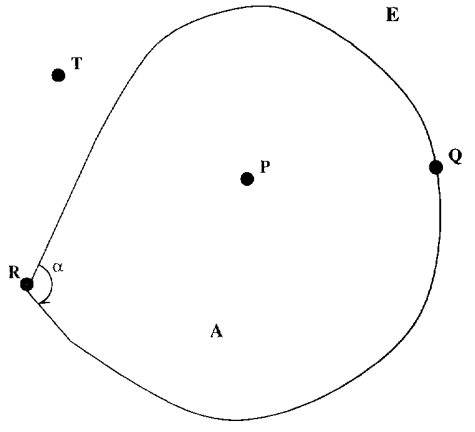

Fig. 1. Domain over which the boundary value problem is defined.

$$C(z)f(z) = \frac{1}{2\pi i}\oint_{\partial A}\frac{h(z')\,dz'}{z'-z} - \frac{1}{\pi}\int_A \frac{g\,dA'}{z'-z} \tag{14}$$

where
$C(z) = 1$ for an internal point like P,
$C(z) = 1/2$ for a point on a smooth portion of the boundary like Q,
$C(z) = \alpha/2\pi$ for corner points like R,
C(z) = 0 for an external point like T.
If the region A is the full space E, the boundary term vanishes if $f(z) \to z^{-\beta}$, as $|z| \to \infty$, where $\mathrm{Re}\,(\beta) > 0$. The solution to the above problem then becomes,

$$f(z) = -\frac{1}{\pi}\int_E \frac{g(z')\,dA'}{(z'-z)}. \tag{15}$$

In steady state problems, we are mostly interested in cases where the function, g, is expressible as $g = P_{,x}$, where P is a complex function. Further, we are interested in situations where $P \equiv 0$, in $\bar{A}^C$, the complement of some region A in E. In this case as shown in Wu and Hui (1987) the theory of distributions as described in Schwartz (1966), may be employed to obtain

$$f(z) = -\frac{1}{\pi}\int_A \frac{P_{,x'}\,dA'}{z'-z} + \frac{1}{\pi}\oint_{\partial A}\frac{P\,dy'}{(z'-z)}. \tag{16}$$

2.2. *The equations of steady state plane elastodynamics in complex form*

To apply the theory of generalized analytic functions, we express the governing field equations in complex form. We define the following scaled coordinates and operators.

$$z_1 = x + i\alpha_1 y, \quad z_2 = x + i\alpha_2 y$$

$$\partial_{z_1} = \frac{1}{2}\left[\partial_x + \frac{i}{\alpha_1}\partial_y\right], \quad \partial_{z_2} = \frac{1}{2}\left[\partial_x + \frac{i}{\alpha_2}\partial_y\right], \tag{17}$$

$$\alpha_1 = \sqrt{1-(v/c_d)^2}, \quad \alpha_2 = \sqrt{1-(v/c_s)^2}, \tag{18}$$

where c_s and c_d are the shear wave speed and longitudinal wave speed respectively. The complex quantities θ and λ defined below completely specify the in plane stress components and hence we shall use them to represent the state of stress,

$$\theta \equiv (\sigma_{xx} + \sigma_{yy})/2, \quad \lambda \equiv (\sigma_{yy} - \sigma_{xx} + 2i\sigma_{xy})/2. \tag{19}$$

The stress-strain relations in isotropic linear elastic materials can be expressed in complex form as

$$\partial_z \bar{U} = \frac{-\lambda}{2\mu}, \tag{20}$$

$$\mathrm{Re}\,(\partial_z U) = \frac{(1-2v)}{2\mu}\theta. \tag{21}$$

where $U = u_x + iu_y$, and u_x, u_y are the Cartesian components of the in plane displacement. In the absence of body forces, the equations of compatibility and momentum balance may be expressed as

$$\partial_{z_1}\partial_{\bar{z}_1}\theta = 0, \tag{22}$$

$$\partial_z^2\theta-\alpha_2^2\,\partial_{z_2}\partial_{z_2}\lambda=0. \tag{23}$$

The compatibility equation implies that θ is the real part of an analytic function, i.e.,

$$\theta=(\alpha_2^2-\alpha_1^2)(\phi(z_1)+\overline{\phi(z_1)}), \tag{24}$$

where $\phi(z_1)$ is analytic. To determine the general solution to the momentum balance equation (23), we define λ as

$$\lambda\equiv(1+\alpha_1)^2\phi(z_1)+(1-\alpha_1)^2\overline{\phi(z_1)}+\Gamma, \tag{25}$$

where Γ is an unknown complex function. Substituting the above equation into (23) and making use of the following relations

$$\begin{aligned}2\partial_{z_2}&=(\partial_{z_1}+\partial_{\bar z_1})-\frac{\alpha_1}{\alpha_2}(\partial_{z_1}-\partial_{\bar z_1})\\ 2\partial_z&=(\partial_{z_1}+\partial_{\bar z_1})-\alpha_1(\partial_{z_1}-\partial_{\bar z_1}),\end{aligned} \tag{26}$$

eqn (23) reduces to

$$\partial_{z_2}\partial_{\bar z_2}\Gamma=0. \tag{27}$$

The general solution to (27) is

$$\Gamma=(1+\alpha_2)^2f(z_2)+(1-\alpha_2)^2\overline{g(z_2)}, \tag{28}$$

where $f(z_2)$ and $g(z_2)$ are analytic functions of z_2. These functions are however not independent as they are related by the stress-strain law. The analyticity of the functions ϕ,f,g implies that there exist functions L,F and G such that,

$$\partial_{z_1}L=\phi(z_1),\quad \partial_{z_2}F=f(z_2),\quad \partial_{\bar z_2}G=g(z_2). \tag{29}$$

The stress-strain law (20) can be integrated to obtain the displacement according to

$$U=-\frac{1}{\mu}[(1+\alpha_1)\overline{L(z_1)}+(1-\alpha_1)L(z_1)+(1+\alpha_2)\overline{F(z_2)}+(1-\alpha_2)G(z_2)] \tag{30}$$

Substituting the above value of displacement into (21) we obtain,

$$\mathrm{Re}\,[\overline{f(z_2)}+g(z_2)]=0, \tag{31}$$

implying that,

$$f(z_2)=-g(z_2)\equiv\psi(z_2), \tag{32}$$

where ψ is some analytic function. Thus we have shown that the in-plane stresses for steady state elastodynamic problems without body force loading are uniquely determined by two analytic functions $\phi(z_1)$ and $\psi(z_2)$ as follows:

$$\theta=(\alpha_2^2-\alpha_1^2)(\phi(z_1)+\overline{\phi(z_1)}), \tag{33}$$

$$\lambda=(1+\alpha_1)^2\phi(z_1)+(1-\alpha_1)^2\overline{\phi(z_1)}+(1+\alpha_2)^2\psi(z_2)-(1-\alpha_2)^2\overline{\psi(z_2)}. \tag{34}$$

The equivalence between the stress functions ϕ and ψ and the complex quantities λ and θ and the in plane stress components is as follows,

$$\phi, \psi \overset{(33,34)}{\Longrightarrow} \theta, \lambda \overset{(19)}{\Leftrightarrow} \underline{\sigma} \tag{35}$$

In view of the complexity involved in representing this problem mathematically, these three sets of quantities will be used interchangeably to represent the state of stress. This equivalence also holds for fictitious stresses that will be defined later.

If body forces are present, eqns (22, 23) are inhomogeneous. As shown in Kallivayalil (1995), in the case of infinite bodies, where the body forces are present in a bounded region, the inhomogeneous equations can be solved by finding solutions to equations of the form

$$\partial_{z_1}\phi = AF_1, \quad \phi \to 0, \quad \text{as } |z_1| \to \infty \tag{36}$$

$$\partial_{z_2}\psi = -BF_2, \quad \psi \to 0, \quad \text{as } |z_2| \to \infty \tag{37}$$

where

$$F_1 \equiv f_x + i\alpha_1 f_y, \quad F_2 \equiv \alpha_2 f_x + i f_y, \quad A = \frac{1}{4(1-\alpha_2^2)\alpha_1^2}, \quad B = \frac{1}{4(1-\alpha_1^2)\alpha_2^2}, \tag{38}$$

and f_x and f_y are the Cartesian components of the body force distribution. The above equations are in the form of (12) and can be solved as described in subsection 2.1.

3. FORMULATION OF PROBLEM

The stress field, $\underline{\sigma}$, may be obtained as the superposition of three problems as illustrated in Fig. 2. The three problems are:

(i) The square root singular stresses that develop in a linear elastic body due to the motion of a crack at constant velocity, v, characterized by the applied dynamic stress intensity factor K_I^A. These stresses will be denoted by $\underline{\sigma}^{el}$, and are calculated in terms of the stress functions ϕ^A, ψ^A defined below. The small scale yielding condition implies that the crack can be modeled as semi-infinite with the tractions specified by the dynamic stress intensity factor, K_I^A, as $r \to \infty$. The stress fields characterized by the dynamic stress intensity factor, K_I^A, for steady crack growth are given in Freund (1990). The corresponding stress functions ϕ^A and ψ^A are

$$\phi^A(z_1) = \frac{-(1+\alpha_2^2)K_I^A}{\Delta\sqrt{2\pi z_1}}, \quad \psi^A(z_2) = \frac{2\alpha_1 K_I^A}{\Delta\sqrt{2\pi z_2}}, \tag{39}$$

where Δ is defined as

$$\Delta \equiv 2[4\alpha_1\alpha_2 - (1+\alpha_2^2)^2]. \tag{40}$$

(ii) The self stress due to inelastic effects modeled as an inhomogeneity moving through an infinite uncracked body with constant velocity 'v'. These stresses are denoted by $\underline{\sigma}^s_{uc}$ and will be calculated in terms of λ^s_{uc} and θ^s_{uc}. The subscript uc denotes an uncracked body.

(iii) The image stresses induced by releasing the tractions due to the self stress problem on the prospective crack plane. These stresses will be denoted by $\underline{\sigma}^{im}$ and will be calculated in terms of ϕ^{im} and ψ^{im}.

Solutions to problems 2 and 3 are now discussed.

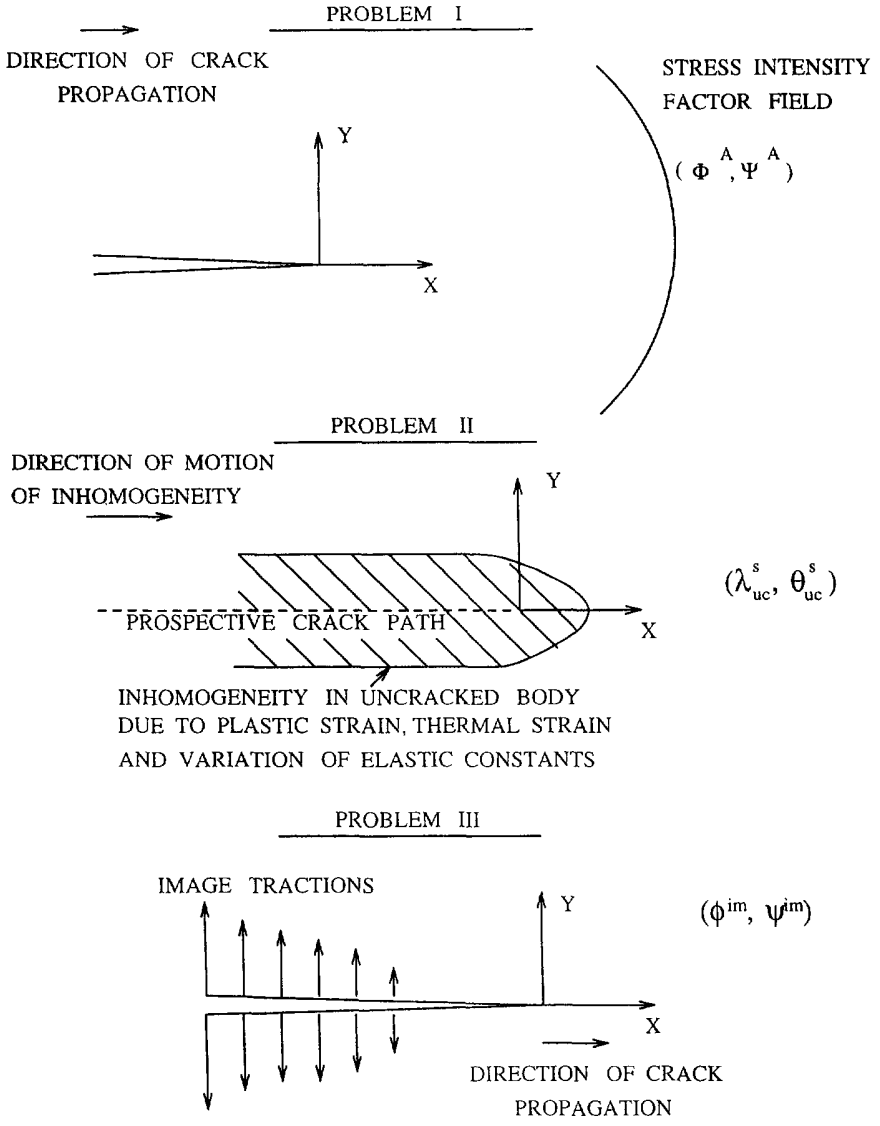

Fig. 2. Superposition of problems.

3.1. *Solution to problem* 2

The self stress $\underline{\sigma}^s_{uc}$, induced by an inhomogeneity moving at constant velocity through the uncracked body, is solved for using the results from Section 2.1. Any departure from a linear elastic, homogeneous, isotropic state at a fixed reference temperature T_o is considered an inhomogeneity. Thus the effects due to plastic flow, variation in material properties due to a temperature field, thermal expansion or even a prescribed state of incompatible strain are all referred to collectively as inhomogeneities. These inhomogeneities are represented as fictitious body forces in a manner that is described now. All fictitious quantities are represented as starred quantities.

The stress tensor is related to the elastic strain tensor by

$$\underline{\sigma} \equiv \underline{\underline{C}}(T) : \underline{\varepsilon}^e \tag{41}$$

where $C(T)$ is the temperature dependent elasticity tensor. The stress may alternatively be expressed as

$$\underline{\sigma} = (\underline{\underline{C}}(T_o) - [\underline{\underline{C}}(T_o) - \underline{\underline{C}}(T)]) : (\underline{\varepsilon} - \underline{\varepsilon}^{pl} - \underline{\varepsilon}^{th}). \tag{42}$$

Further we define the following fictitious stresses:

$$\underline{\sigma}^*_{uc} = \underline{\underline{C}}(T_o) : \underline{\varepsilon}, \quad \underline{\sigma}^{*inh}_{uc} = \underline{\underline{B}}(T) : \underline{\varepsilon}^e, \quad \underline{\sigma}^{*pl}_{uc} = \underline{\underline{C}}(T_o) : \underline{\varepsilon}^{pl}, \quad \underline{\sigma}^{*th}_{uc} = \underline{\underline{C}}(T_o) : \underline{\varepsilon}^{th}, \tag{43}$$

where $\underline{\underline{B}}$ is the difference between the elasticity tensor at the reference temperature and the elasticity tensor at a given temperature T,

$$\underline{\underline{B}}(T) = \underline{\underline{C}}(T_o) - \underline{\underline{C}}(T). \tag{44}$$

The state of self stress $\underline{\sigma}^s_{uc}$, may be expressed in terms of the fictitious stresses as

$$\underline{\sigma}^s_{uc} = \underline{\sigma}^*_{uc} - \underline{\sigma}^{*inh}_{uc} - \underline{\sigma}^{*pl}_{uc} - \underline{\sigma}^{*th}_{uc}. \tag{45}$$

The momentum balance equation may be expressed as

$$\nabla \cdot \underline{\sigma}^*_{uc} - \underbrace{\nabla \cdot \overbrace{\underline{\underline{B}}(T) : \underline{\varepsilon}^e}^{\underline{\sigma}^{*inh}_{uc}}}_{\mathbf{f}^*_{inh}} - \underbrace{\nabla \cdot \overbrace{\underline{\underline{C}}(T_o) : \underline{\varepsilon}^{pl}}^{\underline{\sigma}^{*pl}_{uc}}}_{\mathbf{f}^*_{pl}} - \underbrace{\nabla \cdot \overbrace{\underline{\underline{C}}(T_o) : \underline{\varepsilon}^{*th}}^{\underline{\sigma}^{*th}_{uc}}}_{\mathbf{f}^*_{th}} + \mathbf{f}_a = \rho \frac{\partial^2 \mathbf{u}}{\partial t^2}, \tag{46}$$

where
$\mathbf{f}^*_{inh}$ is the fictitious body force representing the effect of the variation in elastic properties due to a temperature field,
$\mathbf{f}^*_{pl}$ is the fictitious body force representing the effect of plastic flow,
$\mathbf{f}^*_{th}$ is the fictitious body force representing the effect of thermal expansion, and $\mathbf{f}_a$ is the applied body force loading.

In this work we shall assume that there are no applied body forces. Thus total fictitious body force acting on the body is

$$\mathbf{f}^* = -(\mathbf{f}^*_{inh} + \mathbf{f}^*_{pl} + \mathbf{f}^*_{th}). \tag{47}$$

The fictitious stress $\underline{\sigma}^*_{uc}$, induced in the body E (see Fig. 2) due to the fictitious body forces is obtained using (15, 36–38)

$$\phi^*_{uc}(z_1) = -\frac{A}{\pi} \int_\Omega \left(\frac{F^*_1(z'_1)\, \mathrm{d}A'}{(z'_1 - z_1)} \right), \quad \psi^*_{uc}(z_2) = \frac{B}{\pi} \int_\Omega \left(\frac{F^*_2(z'_2)\, \mathrm{d}A'}{(z'_2 - z_2)} \right), \tag{48}$$

where the subscript *uc* implies that the quantity corresponds to the uncracked body. In eqn (48) the region Ω is the region containing the inhomogeneity as shown in Fig. 2. If the region Ω is bounded, the boundary conditions of the original problem do not have to be modified. In the case of dynamic fracture, the region Ω is unbounded due to the plastic wake region trailing the crack. This means that the boundary conditions have to be modified by the fictitious tractions $-\underline{\underline{C}} : \underline{\varepsilon}^i \mathbf{n}$, on the portion of the boundary $\partial\Omega_1$ as indicated

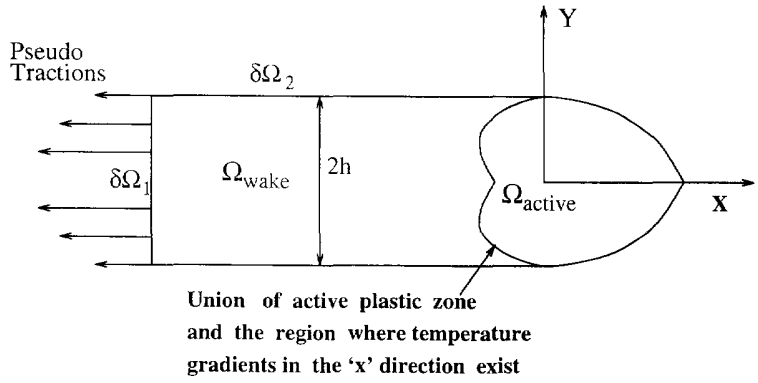

Fig. 3. Schematic of inhomogeneity moving through uncracked body.

schematically in Fig. 3. However in this study we shall ignore the effect of these boundary tractions by not including the contribution from the portion of the boundary $\partial\Omega_1$ to the stress functions ϕ^*_{uc} and ψ^*_{uc}. In Section 3, the effect of ignoring these boundary tractions is discussed.

To facilitate the analysis of rate dependent materials, it is convenient to represent the body forces as follows. From the definition of the operator ∂_{z_i}, the partial derivatives with respect to y, may be expressed as,

$$\partial_y = \alpha_1(i\partial_x - 2i\partial_{z_1}) = \alpha_2(i\partial_x - 2i\partial_{z_2}). \tag{49}$$

Since the body forces are expressed in terms of partial derivatives of x and y, the above relation may be used to express the body forces in terms of partial derivatives of x and the operator ∂_{z_i}. The steady state condition allows us to then express the partial derivatives with respect to x in a moving co-ordinate frame in terms of the crack velocity and the material derivative from (3). These quantities will be referred to as active quantities. Terms involving the partial differential operators ∂_{z_1} or ∂_{z_2} are referred to as residual quantities. Thus F^*_1 and F^*_2 can be rewritten as

$$F^*_1 = g_1 + \partial_{z_1}(residual_1), \quad F^*_2 = g_2 + \partial_{z_2}(residual_2), \tag{50}$$

where the quantities g_1, g_2, $residual_1$ and $residual_2$ are given in Kallivayalil (1995). In evaluating ϕ^*_{uc}, ψ^*_{uc} by substituting (50) in (48), it is convenient to decompose the region Ω shown in Fig. 3, into Ω_{active} and Ω_{wake}. The region where $|g_1|, |g_2| > 0$, is denoted by Ω_{active}, while Ω_{wake} is the region behind the active region where $g_1, g_2 = 0$, and only residual quantities exist. Using eqns (48, 50) the stress functions ϕ^*_{uc}, ψ^*_{uc} for the fictitious stress $\underline{\sigma}^*_{uc}$ may be expressed as the sum

$$\phi^*_{uc} = \phi^{active} + \phi^{residual}, \quad \psi^*_{uc} = \psi^{active} + \psi^{residual}, \tag{51}$$

$$\phi^{active}(z_1) = A\int_{\Omega_{active}} \frac{g_1(z'_1)\,dA'_1}{z'_1 - z_1} \quad \psi^{active}(z_2) = B\int_{\Omega_{active}} \frac{g_2(z'_2)\,dA'_2}{z'_2 - z_2}, \tag{52}$$

where

$$\frac{dA'_1}{\alpha_1} = \frac{dA'_2}{\alpha_2} = dx\,dy \tag{53}$$

and A, B are defined in eqn (38). The residual terms can be evaluated using (14), with g replaced by $\partial_{z_i}(residual_i)$ and h replaced with $(residual_i)$. The contribution from the portion

$\partial\Omega_2$ of the boundary of the inhomogeneity shown in Fig. 3 vanishes, since the plastic strain and temperature difference vanish on $\partial\Omega_2$. However, the contribution from the portion $\partial\Omega_1$

$$\lim_{x'\to-\infty}\frac{1}{2\pi i}\int_{-h}^{h}\frac{(residual_j(z_j'))\,dy'}{(z_j'-z_j)}\quad j\to 1,2 \tag{54}$$

does not vanish. For points in the vicinity of the crack tip, if the functions $residual_j(z_j)$ are bounded for $y\in[-h,h]$, the contribution from the $\partial\Omega_1$ portion of the boundary to the contour integral in (14) may be ignored and the residual terms are

$$\phi^{residual}=A(residual_1)\quad \psi^{residual}=-B(residual_2). \tag{55}$$

Using eqn (45), the actual self stresses in the uncracked body may be expressed as

$$\theta_{uc}^{s}=\theta^{active}+\overbrace{\theta^{residual}-\theta^{*inh}-\theta^{*pl}-\theta^{*th}}^{\theta^{wake}}, \tag{56}$$

$$\lambda_{uc}^{s}=\lambda^{active}+\overbrace{\lambda^{residual}-\lambda^{*inh}-\lambda^{*pl}-\lambda^{*th}}^{\lambda^{wake}}, \tag{57}$$

where θ, λ are calculated using (33) and (34).

3.2. *Solution to problem* 3

To obtain traction free conditions on the crack faces, we negate the tractions caused by the self stress problem described in the previous subsection, on the line representing the crack face in the uncracked body. This problem is referred to as the image stress problem.

An evaluation of the terms θ^{wake} and λ^{wake} in eqns (56, 57) indicates that

$$\theta^{wake}=-\lambda^{wake} \tag{58}$$

and hence the tractions on the crack face are due to active quantities only.

The tractions on the crack face, $z_1=z_2=t$, $t<0$, are given by

$$-(\sigma_{yy}^{im}(t)+i\sigma_{xy}^{im}(t))=\theta_{uc}^{s}(t)+\lambda_{uc}^{s}(t)=a\phi(t)^{active}+b\overline{\phi(t)}^{active}+c\psi(t)^{active}+d\overline{\psi(t)}^{active}=\Gamma(t), \tag{59}$$

where the constants a, b, c and d are

$$a=1+2\alpha_1+\alpha_2^2\quad b=1-2\alpha_1+\alpha_2^2\quad c=(1+\alpha_2)^2\quad d=-(1-\alpha_2)^2. \tag{60}$$

We define

$$\lim_{\eta\to0,\eta>0}\phi^{im}(x,\eta)=\phi^{+},\quad \lim_{\eta\to0,\eta<0}\phi^{im}(x,\eta)=\phi^{-}. \tag{61}$$

According to the above definitions

$$(\bar{\chi})^{+}=\bar{\chi}^{-}, \tag{62}$$

where χ is any general complex quantity. The traction boundary conditions may hence be expressed as the limiting values of analytic functions as one approaches the crack face, i.e.,

$$
\begin{aligned}
a\phi^{+}+b\tilde{\phi}^{-}+c\psi^{+}+d\tilde{\psi}^{-} &= \Gamma(t) \quad \text{(a)}\\
a\phi^{-}+b\tilde{\phi}^{+}+c\psi^{-}+d\tilde{\psi}^{+} &= \Gamma(t) \quad \text{(b)}\\
b\phi^{+}+a\tilde{\phi}^{-}+d\psi^{+}+c\tilde{\psi}^{-} &= \overline{\Gamma(t)} \quad \text{(c)}\\
b\phi^{-}+a\tilde{\phi}^{+}+d\psi^{-}+c\tilde{\psi}^{+} &= \overline{\Gamma(t)} \quad \text{(d).}
\end{aligned} \tag{63}
$$

Subtracting (b) from (a) and using the fact that we require that the stresses and rotations vanish at ∞, we obtain

$$a\phi^{im}+c\psi^{im}-b\tilde{\phi}^{im}-d\tilde{\psi}^{im}=0. \tag{64}$$

Adding (a) and (b) and using the Plemlj formulae we obtain,

$$a\phi+c\psi+b\tilde{\phi}+d\tilde{\psi}=\frac{1}{\pi i\sqrt{z_i}}\int_{-\infty}^{0}\frac{\Gamma(t)\sqrt{(t)}\,\mathrm{d}t}{(t-z_i)}. \tag{65}$$

The variable z_i is used to indicate that the analytic function can be expressed in terms of z, z_1 or z_2 as they all have the same value on the real line. Similarly using linear combinations of (c) and (d) and solving the resulting equations, the image stress functions ϕ^{im}, ψ^{im} which determine the image stresses are,

$$\phi^{im}(z_1)=\frac{1}{2\pi i\Delta\sqrt{z_1}}\int_{-\infty}^{0}\frac{\sqrt{t}[\mathrm{d}\Gamma(t)-c\overline{\Gamma(t)}]\,\mathrm{d}t}{(t-z_1)}, \tag{66}$$

$$\psi^{im}(z_2)=\frac{1}{2\pi i\Delta\sqrt{z_2}}\int_{-\infty}^{0}\frac{\sqrt{t}[a\overline{\Gamma(t)}-b\Gamma(t)]\,\mathrm{d}t}{(t-z_2)}, \tag{67}$$

where Δ is defined in (40). The condition $\Delta=0$ defines the Rayleigh wave speed, indicating that steady state crack growth is not possible beyond the Rayleigh wave speed in accordance with the results of Stroh (1990).

Using (51), (52) and (59) the image traction at t, due to a point inhomogeneity at z', is given by

$$\Gamma(t)=\frac{-1}{4\pi\alpha_1\alpha_2(1-\alpha_2^2)}\left[\frac{a\alpha_2 g_1(z')}{(t-z_1')}+\frac{b\alpha_2\bar{g}_1(z')}{(t-\overline{z_1'})}-\frac{c\alpha_1 g_2(z')}{(t-z_2')}-\frac{d\alpha_1\bar{g}_2(z')}{(t-\overline{z_2'})}\right]. \tag{68}$$

In order to calculate the image stresses according to eqns (66, 67), we must evaluate integrals of the form

$$I(z,z')=\int_{-\infty}^{0}\frac{\sqrt{t}\,\mathrm{d}t}{(t-z')(t-z)}. \tag{69}$$

As shown in Kallivayalil (1995)

$$I(z,z')=\frac{\pi i}{(\sqrt{z}+\sqrt{z'})}. \tag{70}$$

Substituting (68) into (66), (67) and using (70), the image stress functions are

$$\phi^I(z_1) = \frac{\mu z_1^{-1/2}}{4\pi\alpha_1\alpha_2(1-\alpha_2^2)}\left[\frac{\alpha_2}{\alpha_1}\int_{\Omega_{active}}\frac{g_1[1-e/\Delta]\mathrm{d}A_1'}{(\sqrt{z_1}+\sqrt{z_1'})} + \frac{p}{\Delta\alpha_2}\int_{\Omega_{active}}\frac{g_2\mathrm{d}A_2'}{(\sqrt{z_1}+\sqrt{z_2'})}\right], \quad (71)$$

$$\psi^I(z_1) = \frac{\mu z_2^{-1/2}}{4\pi\alpha_1\alpha_2(1-\alpha_2^2)}\left[-\frac{\alpha_1}{\alpha_2}\int_{\Omega_{active}}\frac{g_2[1-e/\Delta]\mathrm{d}A_2'}{(\sqrt{z_2}+\sqrt{z_2'})} + \frac{p}{\Delta\alpha_1}\int_{\Omega_{active}}\frac{g_1\mathrm{d}A_1'}{(\sqrt{z_2}+\sqrt{z_1'})}\right], \quad (72)$$

where

$$e = 2[4\alpha_1\alpha_2+(1+\alpha_2^2)^2], \quad p = 8\alpha_1\alpha_2(1+\alpha_2^2). \quad (73)$$

3.3. *Stresses in the presence of a moving crack*

Using the results of the previous two subsections a local stress intensity factor may be defined in terms of the stress functions ϕ_{ss} and ψ_{ss}, defined as

$$\phi_{ss} = \phi^I + \phi^{active}, \quad \psi_{ss} = \psi^I + \psi^{active}. \quad (74)$$

The local stress intensity factor, K_{ID}^* is defined as,

$$K_{ID}^* \equiv \lim_{t\to 0^+}[\sqrt{2\pi t}[a\phi_{ss}(t)+b\bar{\phi}_{ss}(t)+c\psi_{ss}(t)+d\bar{\psi}_{ss}(t)]] \quad (75)$$

Thus for a square root singularity to exist at the crack tip, we must have

$$K_{tip} = K_I^A + K_{ID}^* > 0 \quad (76)$$

where K_I^A represents the applied stress intensity factor. There are many instances where the resulting stress intensity factor, K_{tip}, is zero, implying that the elastic square root singular field does not exist at the crack tip, as shown in Achenbach (1979) and Yang (1986). In the next section, we provide a means of evaluating the crack tip stress intensity factor from an energy balance.

3.4. *Modeling of the wake region*

Since the fictitious body forces are defined in terms of the gradients of the inhomogeneity, the active inelastic zone is defined as the region where these gradients exist. This active region is assumed to be of finite extent. In the wake region, the linear elastic fields, characterized by the stress intensity factor, are not dominant. The stress state in the wake region sufficiently far away from the active region is well approximated by the wake terms in eqns (56, 57). Using (45), (33), (34) and (19) the wake terms are computed to be

$$\sigma_{xx}^{wake} = -2\mu(T_o)\left[\varepsilon_{xx}^{pl} - \frac{\nu}{1-\nu}\varepsilon_{yy}^{pl}\right] - \frac{2\mu(T_o)\nu}{1-\nu}\varepsilon_{kk}^{pl}$$
$$2(\mu(T_o)-\mu(T))\left[\varepsilon_{xx}^{e} - \frac{\nu}{1-\nu}\varepsilon_{yy}^{e}\right] - \frac{2(\mu(T_o)-\mu(T))\nu}{1-\nu}\varepsilon_{kk}^{e} - \frac{\mu(T_o)\nu}{(1-\nu)}\alpha\Delta T$$
$$\sigma_{xy}^{wake} = \sigma_{yy}^{wake} = 0. \quad (77)$$

It should be noted that there are stresses only in the x direction as the crack faces are not constrained in the y direction. The state of stress is essentially one of uniaxial compression. The pseudo tractions in Fig. 3 are given by σ_{xx}^{wake}. Since the active zone is assumed to be of finite extent, the pseudo tractions must be such that if they alone were to act on the material, it would not cause yielding in the current state of the material in the wake region. The effect of ignoring these tractions is that the stresses in the wake region may not be calculated accurately. The effect of ignoring these tractions on the stresses in the vicinity of the crack tip is negligible and should a stress intensity factor field exist at

the crack tip, it will be unaffected by ignoring these tractions as they have no opening component.

From a knowledge of stresses in the wake region, the elastic energy density U_e^*, stored in the wake may be determined. This allows us to perform an energy balance for the entire process. As shown in Freund (1990) and Wu (1985), the energy balance for rate dependent materials may be expressed as

$$G_{tip} = G - \frac{1}{v}\int_{\Omega_{active}} \sigma_{ij}\dot{\varepsilon}_{ij}^{pl}\,dA - \int_{-h}^{h} U_e^*(y)\,dy, \tag{78}$$

where G_{tip} represents the crack tip energy release rate and G represents the energy release rate due to the remote stress intensity factor. Further the dynamic stress intensity factor in plane stress may be determined from the energy release rate according to the relation,

$$G_{tip} = \frac{f(v)K_{tip}^2}{E}, \quad f(v) = \frac{v^2\alpha_d}{(1-v)c_s^2 D}. \tag{79}$$

3.5. *Constitutive relations*

During dynamic fracture, the strain rate experienced in the crack tip region may be as high as $10^6\ s^{-1}$ and temperatures at the crack tip may be as high as 500°C, hence constitutive models appropriate for these conditions will have to be used. The strain rate also varies by several orders of magnitude, from $1\ s^{-1}$ to $10^6\ s^{-1}$, hence the mechanisms that are active in influencing the deformation are likely to vary as well. In this work the material is modeled as an elastic-viscoplastic material.

It is assumed that only the shear modulus of the material varies with temperature and that the Poisson's ratio is constant. The isothermal, static stress-strain curve for the material at room temperature is shown in Fig. 4, and the variation of the shear modulus with temperature is shown in Fig. 5, according to Wilson and Esler (1983). A constant Poisson's ratio, determined using ultrasonic techniques at room temperature, of 0.34 is used for the material at all temperatures. The static yield stress variation with temperature is shown in Fig. 6, as determined by Wilson and Esler (1983).

The plastic behavior is modeled as rate dependent, assuming a J_2 flow theory with an associated flow rule. The plastic response is assumed to be isotropic and incompressible. The visco-plastic response is divided into two regimes separated by a transition plastic strain rate, as suggested by Freund (1990). For strain rates below the transition strain rate,

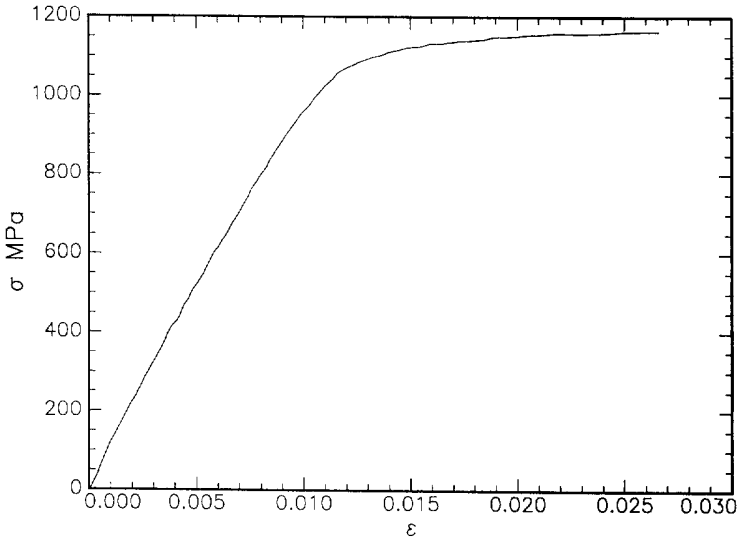

Fig. 4. Static stress-strain curve at room temperature.

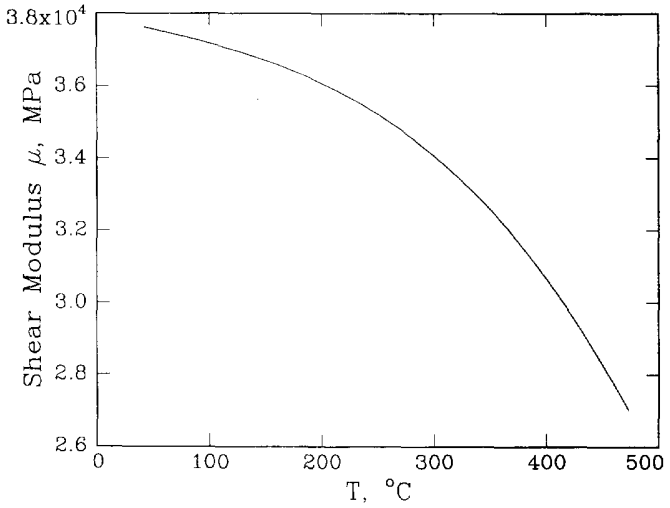

Fig. 5. Variation of shear modulus with temperature.

the thermally activated motion of dislocations past discrete obstacles is assumed to be the rate controlling mechanism, while for strain rates above the transition strain rate, the phonon drag experienced by the dislocations is assumed to be the rate controlling mechanism. The heat treatment given to the alloy results in it being precipitation hardened, thus we believe that the obstacles to dislocation motion will be discrete. The constitutive equation used for the β titanium alloy under consideration is

$$\begin{aligned} \varepsilon_{ij}^{p} &= \left[\dot{\gamma}_t + \dot{\gamma}_o \frac{(\tau-\tau_t)^n}{\mu(T)}\right]\frac{S_{ij}}{2\tau} \quad \tau > \tau_t \\ &= \dot{\varepsilon}_o \exp\left[\frac{-\Delta F}{KT}\left(1-\frac{\tau}{\hat{\tau}}\right)\right]\frac{S_{ij}}{2\tau} \quad \tau_y \leqslant \tau \leqslant \tau_t \\ &= 0 \quad \tau < \tau_y, \end{aligned} \tag{80}$$

where

$\dot{\gamma}_t$ = transition strain rate = $5 \times 10^2\ s^{-1}$ for metals,

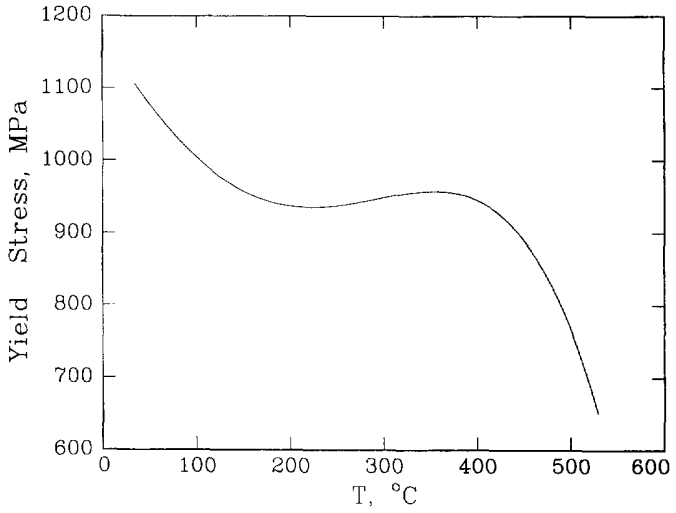

Fig. 6. Static stress-strain curve at room temperature.

$\dot{\gamma}_o$ = phonon drag coefficient = 5×10^6 s^{-1} for metals,
τ_t = temperature dependent stress that results in transition strain rate,
$\mu(T)$ = temperature dependent shear modulus,
n = strain rate sensitivity index,
$\dot{\varepsilon}_o$ = frequency factor for dislocation motion $\approx (10^6$–$10^7)$ for metals
ΔF = activation energy for discrete strong obstacles in β-titanium,
K = Boltzmann's constant, $\Delta F/K \approx 8000$°C,
$\hat{\tau}$ = shear yield strength at absolute zero ≈ 1900 MPa,
τ_y = temperature dependent static yield strength,
$\tau = (\frac{1}{2} S_{ij} S_{ij})^{1/2}$ second invariant of deviatoric stress tensor,
T = absolute temperature.

The transition stress is chosen such that it is above the static yield strength in shear at all temperatures and below the shear strength at absolute zero temperature. The activation energy is estimated from the values provided by Frost and Ashby (1985) for β-titanium. Modeling the precipitates as strong obstacles, a lower bound suggested by Frost and Ashby for the shear yield strength at absolute zero is,

$$\hat{\tau} = \frac{\mu b}{l}, \tag{81}$$

where l is the mean spacing of the discrete obstacles and b the Burgers vector for the slip system. The activation energy ΔF may also be estimated according to Frost and Ashby (1985) as

$$\Delta F \approx \mu b^3. \tag{82}$$

4. NUMERICAL RESULTS

The details of the numerical procedure are described in detail in Wu (1985) and are not repeated here. The following normalizations are used in presenting the results:

$$\hat{x}_i = x_i / \left(\frac{K_I^2}{\sigma_o^2} \right), \quad i = 1, 2$$

$$\hat{\varepsilon}_{ij} = \varepsilon_{ij} / (\sigma_o / E), \quad i, j = 1, 2, 3$$

$$\hat{\sigma}_{ij} = \sigma_{ij} / \sigma_o, \quad i, j = 1, 2, 3$$

$$\hat{\dot{\varepsilon}}_{ij} = \frac{\dot{\varepsilon}_{ij} K_I^2 E}{\sigma_o^3 v}, \quad i, j = 1, 2, 3.$$

Temperature is not normalized and is expressed using the Kelvin scale. Numerical results reflecting the influence of temperature, rate sensitivity and material inertia are presented in this section. Rate sensitivity is characterized by the rate sensitivity index n, and material inertia characterized by the mach number m, which is the ratio of the crack velocity to the shear wave velocity. These results are from a mesh in which 218 constant elements were used. The smallest element at the crack tip was 1/1500 of the overall plastic zone size. Since there are no benchmark problems to compare our solutions to, we use the following tests as checks for the solution:

1) the stress field ahead of the crack should asymptotically approach the stress intensity factor field;
2) the crack faces should be traction free;

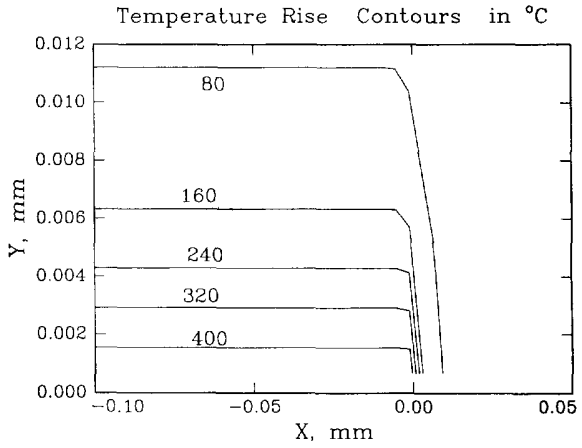

Fig. 7. Imposed temperature field, crack tip is located at (0,0); temperature rise contours in °C.

3) the state of stress in the wake region should not result in yielding.

The temperature field that we impose at the crack tip is shown in Fig. 7 and is such that the maximum temperature rise at the crack tip is 450°C. This value of maximum temperature was selected as it is representative of the temperatures actually measured in this material during dynamic fracture as reported in Kallivayalil *et al.* (1994).

4.1. *Opening stress*

The variation in the opening stress σ_{yy} on a line ahead of the crack with temperature effects included is shown in Fig. 8. The opening stress without temperature effects is

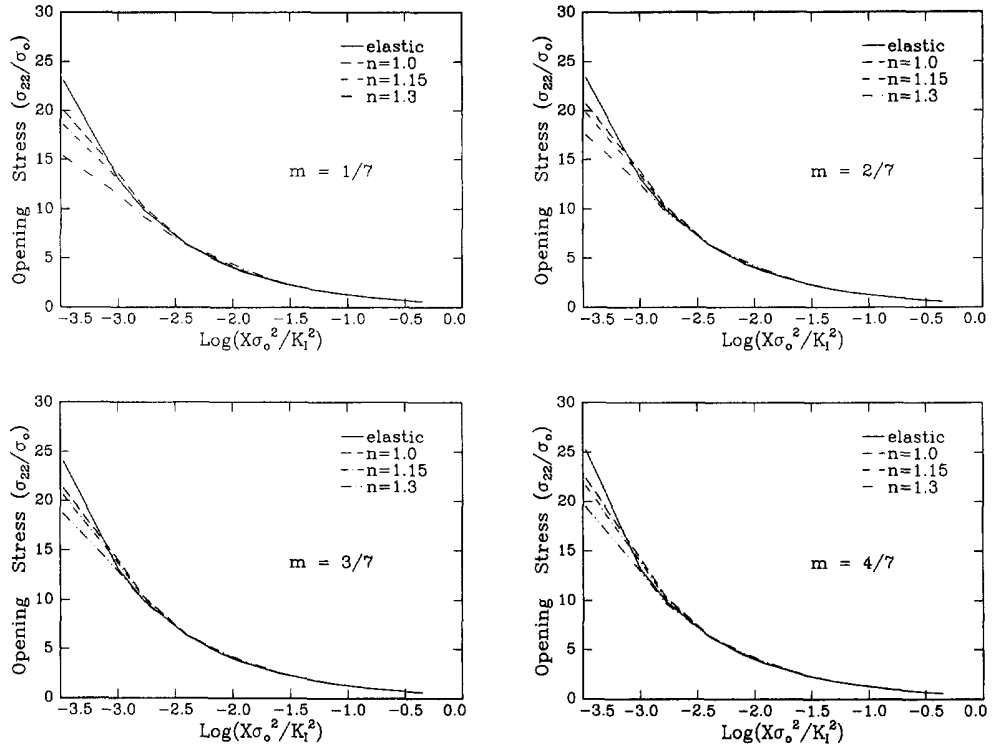

Fig. 8. Variation of opening stress with temperature effects included $K_I = 50$ MPam$^{1/2}$, $\sigma_o = 1100$ MPa, $\dot{\gamma}_o = 5 \times 10^6$ s^{-1}.

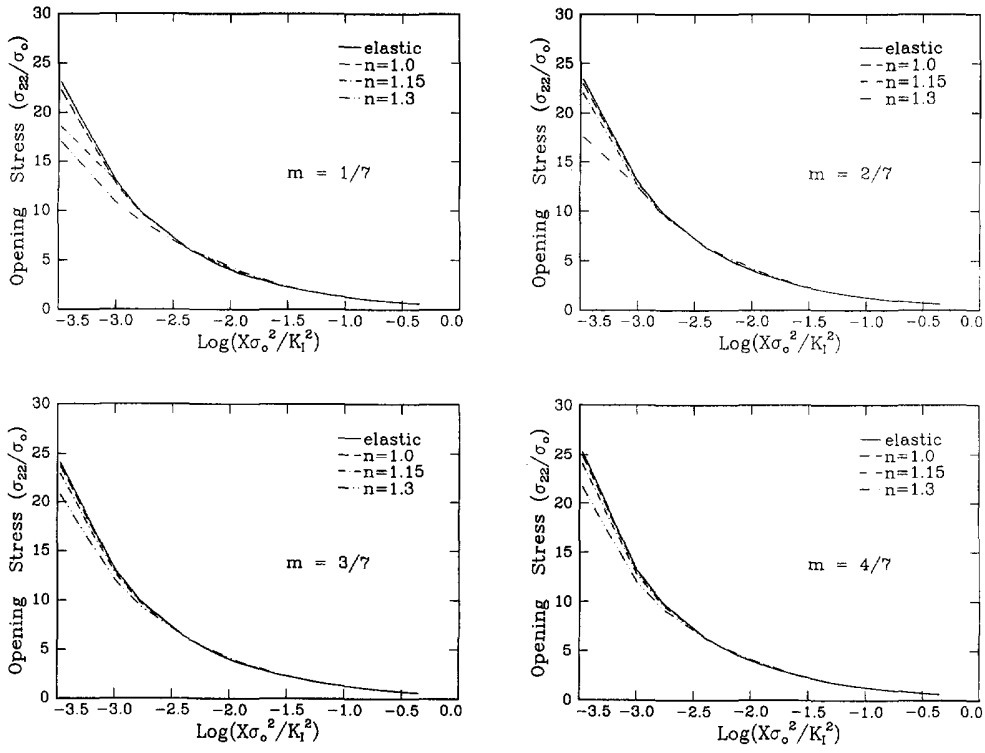

Fig. 9. Variation of opening stress under isothermal conditions $K_I = 50$ MPam$^{1/2}$, $\sigma_o = 1100$ MPa, $\dot{\gamma}_o = 5 \times 10^6$ s^{-1}.

presented in Fig. 9. Comparing the corresponding curves in Figs 8 and 9 to each other it is found that the effect of temperature rise is to lower the opening stresses in the vicinity of the crack tip. In all cases it was verified that the stress field approaches the elastic stress intensity factor field. In comparing the effects of rate sensitivity, the lowering of stress is greatest when the material is less rate sensitive, i.e. as n increases. The effect of material inertia is to prevent stress relief through plastic flow and hence the drop in opening stress decreases as the crack speed increases. These results are consistent with the isothermal analysis at room temperature of Krishna Kumar *et al.* (1989a).

4.2. *Opening plastic strain rate and plastic strain*

The opening strain rate on a line ahead of the crack is shown in Figs 10 and 11. The order of magnitude of the strain rates in the crack tip region is 10^6–10^7 s^{-1}, which is typical of values reported in Krishna Kumar (1989a). For a fixed loading condition represented by a fixed K_I value, the strain rates ahead of the crack increase as the strain rate sensitivity index increases or as the material becomes less rate sensitive. As would be expected, the strain rates are higher for greater mach numbers. The effect of temperature is to lower the strain rate. This result at first seems contradictory, considering the fact that the strain rate increases with decreasing strain rate sensitivity, and increasing the temperature has a similar effect to decreasing strain rate sensitivity. The lowering of strain rates when temperature effects are included is because of the lowering of stresses in the crack tip region caused by the lowering of elastic constants with temperature.

In Fig. 12 the plastic component of the opening strain ahead of the crack is examined. Only the curve with temperature effects is presented as the effects of temperature on strain are identical to its effects on the strain rate for a steady state problem. The maximum opening strain is about 10 times the yield strain and hence about 10%. Thus even though the strain rates are high the total accumulated plastic strain is not large. The effects of inertia are evident in the reduction of the opening plastic strain with increasing crack velocity. Though the strain rates ahead of the crack are higher at greater crack velocity, the

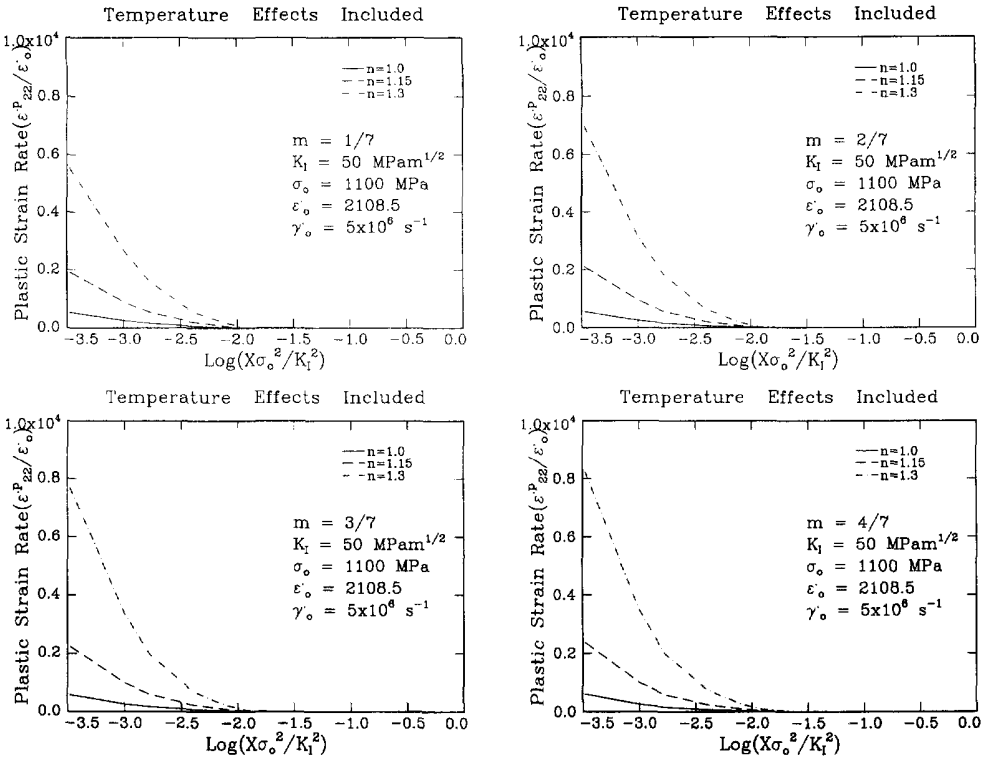

Fig. 10. Variation of plastic strain rate with temperature effects included $K_I = 50$ MPam$^{1/2}$, $\sigma_o = 1100$ MPa, $\dot{\gamma}_o = 5 \times 10^6$ s^{-1}, $\dot{\varepsilon}_o = 2108.5$ s^{-1}.

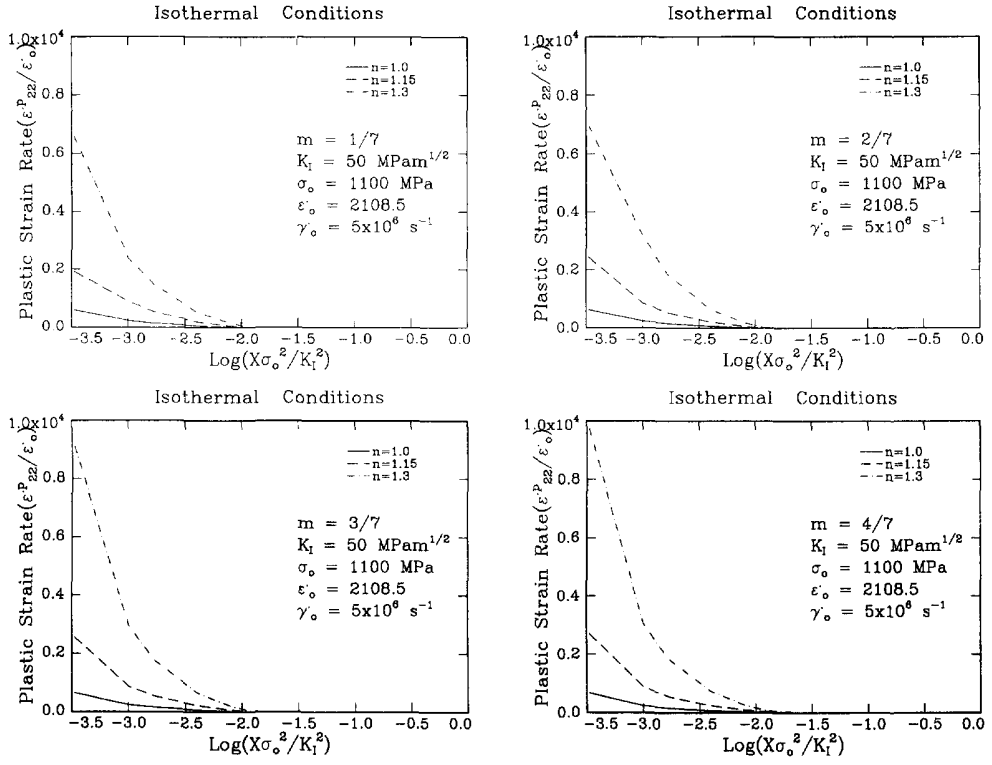

Fig. 11. Variation of plastic strain rate under isothermal conditions $K_I = 50$ MPam$^{1/2}$, $\sigma_o = 1100$ MPa, $\dot{\gamma}_o = 5 \times 10^6$ s^{-1}, $\dot{\varepsilon}_o = 2108.5$ s^{-1}.

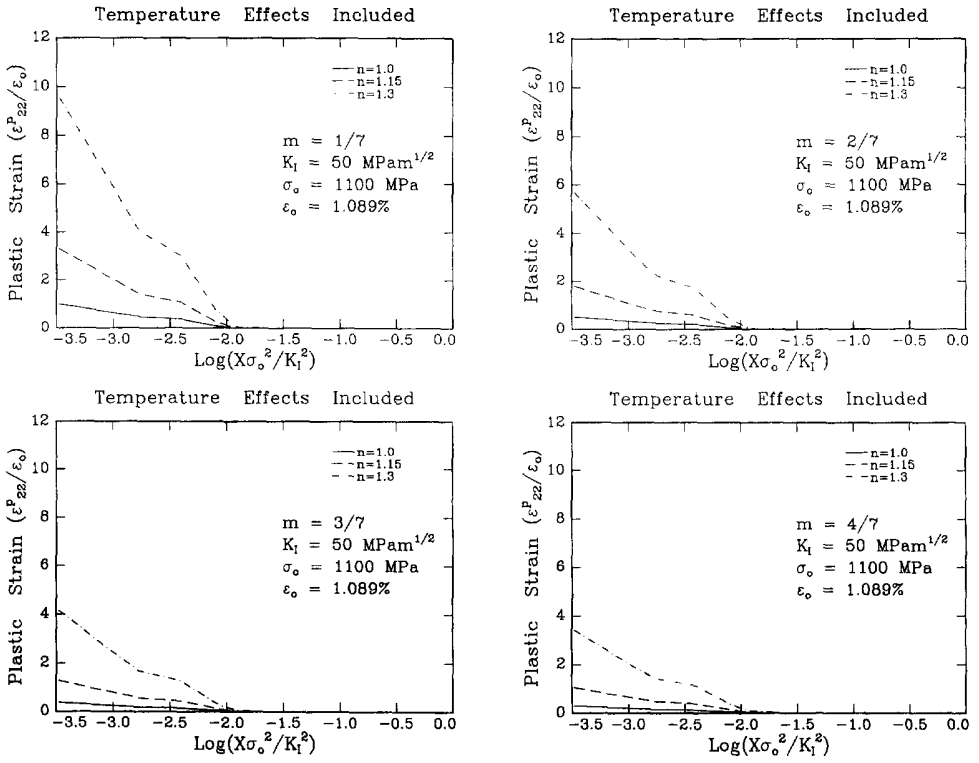

Fig. 12. Variation of plastic strain with temperature effects included $K_I = 50$ MPam$^{1/2}$, $\sigma_o = 1100$ MPa, $\dot{\gamma}_o = 5 \times 10^6$ s^{-1}, $\varepsilon_o = 1.089\%$.

time during which a material point is subjected to loading decreases and hence the plastic strain experienced is lower as the crack velocity increases. The curves corresponding to lower strain rate sensitivity indexes lie below those with higher indexes, demonstrating that the effect of increasing rate sensitivity is to lower the plastic strain.

4.3. *Elastic rate dominance*

The material behavior as one approaches the crack tip, $r \to 0$, is of power law type when $n < 3$. Hence using the same arguments as Hui and Riedel (1981), the elastic strain rates must dominate the plastic strain rates if a square root singularity exists at the crack tip. Figure 13 plots the ratio of the norm of the plastic strain rate to the norm of the elastic strain rate as a function of position ahead of the crack tip. It can be observed that as one approaches the crack tip, the elastic rates dominate initially as one is in the elastic region, then the rates become comparable as one approaches the plastic region and finally the elastic rates dominate again at the crack tip. The figures also indicate that as the material becomes less rate sensitive, i.e. n increases, the region over which the elastic strain rates dominate, becomes smaller and shrinks towards the crack tip, as the curves for $n = 1.3$, lie above the others.

4.4. *Extent of plastic zone*

The plastic zone is partitioned into a high strain rate region where the effective plastic strain rate is greater than the transition strain rate and the low strain rate region where the effective strain rate is less than the transition strain rate. In this example, the transition strain rate was taken to be 1000 s^{-1}. The effect of inertia here is to enlarge the plastic zone and also the high strain rate region. Similar effects have been reported by Krishna Kumar *et al.* (1989b) for rate dependent non-hardening materials and by Deng (1990) for hardening and non-hardening rate independent material. The effect of rate sensitivity is seen in the presence of the reloading zone. For values of strain rate sensitivity index up to $n = 1.15$, no reloading zone was observed, but at a value of $n = 1.3$, a reloading zone begins to

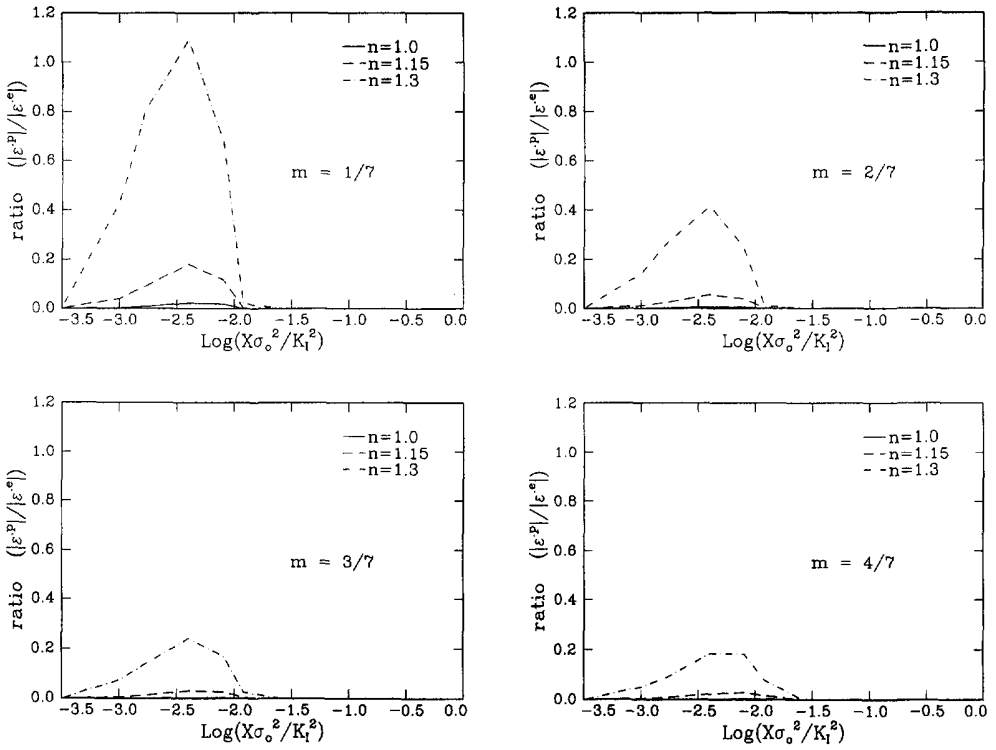

Fig. 13. Ratio of plastic strain rates to elastic strain rates with temperature effects included $K_I = 50$ MPam$^{1/2}$, $\sigma_o = 1100$ MPa, $\dot{\gamma}_o = 5 \times 10^6$ s^{-1}.

appear. The primary loading zone, however, is similar for all of the values of n that were considered. The region of high strain rate is much smaller than the overall plastic zone and has dimensions which are about a tenth of the dimensions of the overall plastic zone.

4.5. *Dynamic stress intensity factors*

The relations between dynamic stress intensity factor and velocity are computed using both ductile and brittle fracture criteria. The brittle criterion is enforced by requiring that the opening stress at a fixed distance ahead of the crack be a critical value, σ_{cr}, for sustained crack growth. Similarly the ductile criterion is enforced by requiring that the critical opening strain at a fixed distance be a critical value, γ_{cr}. The ductile and brittle criteria are imposed at the same distance of 2 μm ahead of the crack. This distance is well within the high strain rate region for the values of stress intensity factor and crack velocities considered here. The critical value of opening stress ahead of the crack, σ_{cr}, for brittle fracture was taken to be 11 times the static yield stress. The critical opening plastic strain for ductile fracture, γ_{cr} was taken to be 3.5 times the static yield strain at room temperature corresponding to the total strain at failure in a tensile test as shown in Fig. 14. The critical stress value is typical of values used in Krishna Kumar (1989c). In calculating K_I^A vs v curves, an initial guess of the required K_I^A is made and then depending on whether a brittle criterion or a ductile criterion is used, the opening stress σ_{yy} or opening plastic strain ε_{yy}^p are determined respectively and compared to the critical value σ_{cr} or γ_{cr}, the value of K_I^A is then increased or decreased until the opening stress or opening plastic strain is within one percent of the critical value.

The following observations may be deduced from Fig. 15. The effect of temperature when the brittle criterion is imposed is to enhance the fracture toughness at all velocities and for all strain rate sensitivity values. It is worth noting that the curvature of the curves obtained for a rate dependent material using the ductile failure criterion is very different from that of the rate insensitive case. As shown in Deng (1990) the rate independent case results in curves that are concave upwards, while for the rate dependent case, Krishna Kumar (1989a) and Freund (1983) have obtained curves that are concave downwards. In

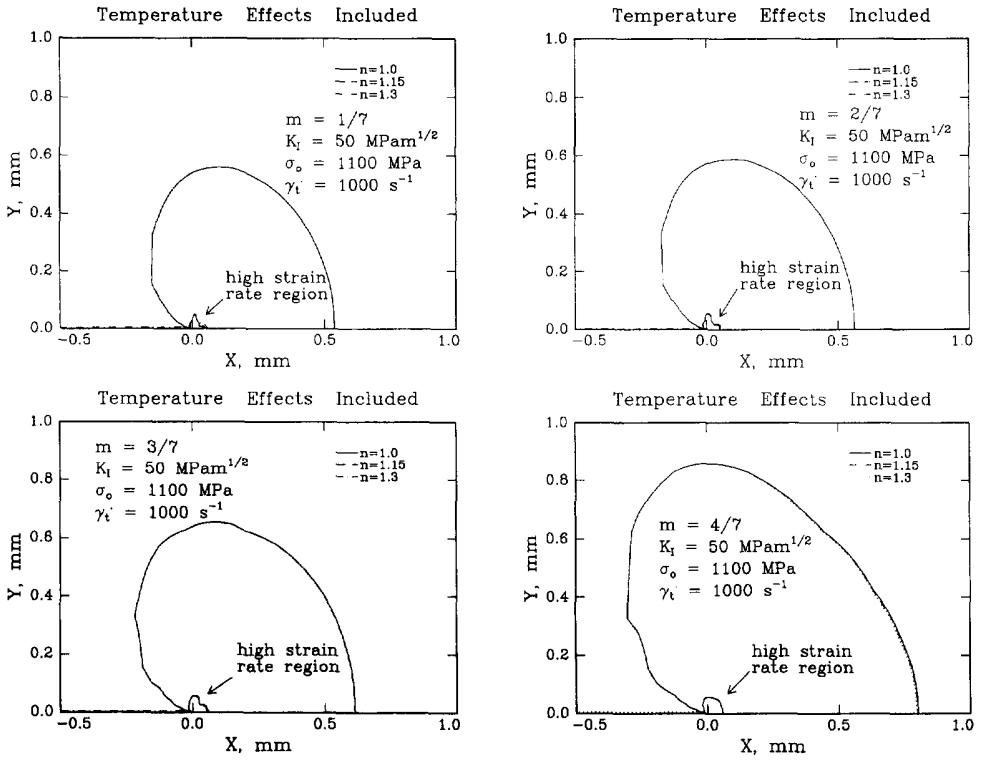

Fig. 14. Variation of plastic zone shapes with temperature effects included $K_I = 50$ MPam$^{1/2}$, $\sigma_o = 1100$ MPa, $\dot{\gamma}_o = 5 \times 10^6$ s^{-1}, $\dot{\gamma}_t = 1000$ s^{-1}.

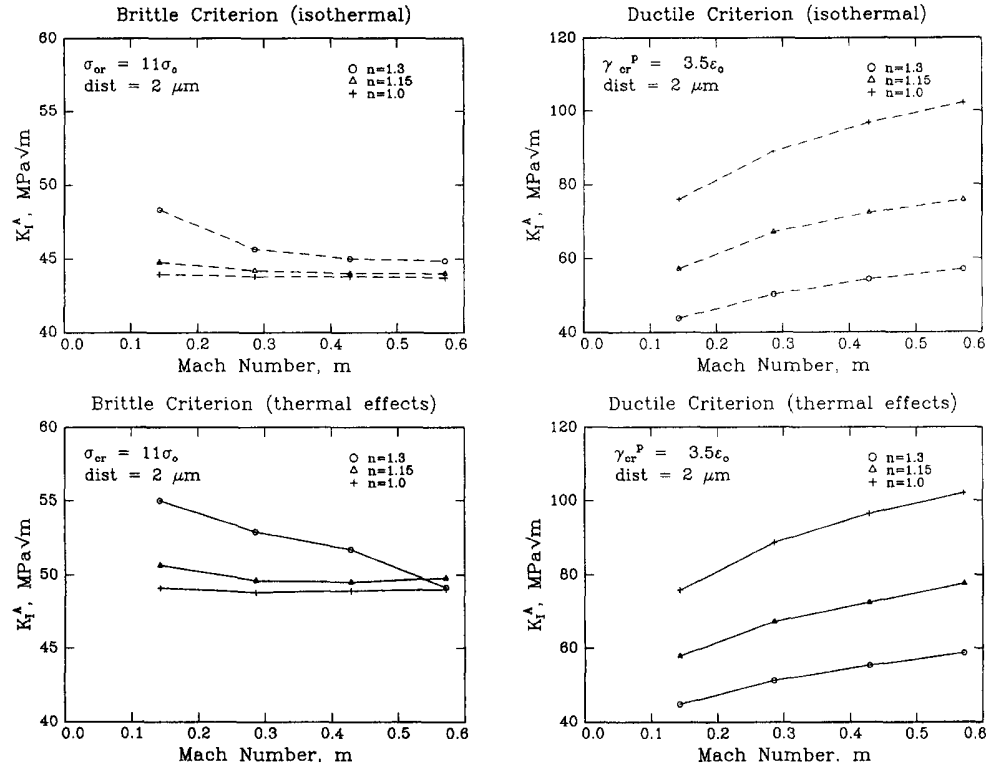

Fig. 15. Relation between dynamic stress intensity factor and velocity.

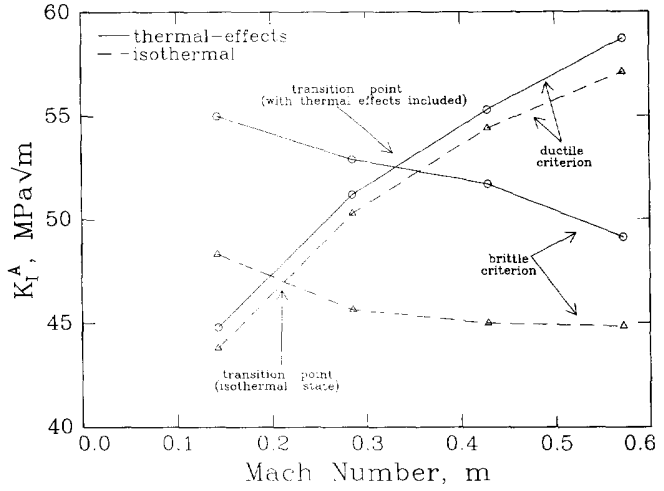

Fig. 16. Ductile-brittle mode transition $n = 1.3$, $\varepsilon_{cr}^{p} = 3.5\varepsilon_{o}$, $\sigma_{cr} = 11\sigma_{o}$.

either case the required value of stress intensity factor for sustained crack growth increases as crack velocity increases. The effect of rate sensitivity is that using a ductile criterion it enhances the fracture toughness while for a brittle criterion it decreases toughness.

In order to study possible fracture mode transitions from ductile to brittle, the two criteria are plotted together in Fig. 16 for $n = 1.3$. The K_I^A vs v relationship is determined at each velocity by whichever criterion is satisfied first. The effect of the crack tip temperature rise is to enhance the fracture toughness at lower velocities and to increase the velocity at which the ductile to brittle transition may occur.

5. CONCLUSIONS

A method for simulating the effects of temperature on dynamic steady state crack growth in a rate dependent material has been developed. The results indicate that the effect of temperature is to provide stress relief at the crack tip, and thus an isothermal analysis incorporating just the effects of rate dependent plasticity over estimates the stresses at the crack tip. The decrease in strain rate when temperature effects are included may be attributed to the drop in elastic modulus with temperature, indicating that the effect of temperature on the elastic constants may be as important as the effect of temperature on the plastic properties of the material. It should be noted that the temperature field obtained from the numerically determined stress and strain rate fields need not be the same as the temperature field imposed. For the constitutive relation and crack growth criteria used, the dynamic fracture toughness of the material is slightly enhanced by the presence of the temperature field at the crack tip. This is especially true when the brittle criterion is imposed. A more dramatic effect is the shift of the transition point from ductile to brittle fracture modes to higher velocities when temperature effects are included. The above conclusions regarding fracture toughness were arrived at by imposing a temperature field that did not vary with crack velocity and will have to be reevaluated if a temperature field dependent on crack velocity is imposed. The accumulated plastic strain may be used as a criterion for the existence of a reverse yielding zone as discussed in the section on modeling the wake. For sufficiently low strain rate sensitivity, i.e. large n, we find that a reverse yielding zone does exist. Further it has been demonstrated that ignoring the unknown boundary conditions in the wake region behind the crack tip does not affect a stress intensity field at the crack tip.

Acknowledgements—The computations were performed using the multiuser computing facility of the Materials Science Center at Cornell University, funded under the MRL program of the NSF, award # DMR-9121654.

REFERENCES

Achenbach, J. D., Burgers, P. and Dunayevsky, V. (1979). Near tip deformation in dynamic fracture problems. *ASME-AMD* **35,** 105–124.

Deng, X. (1990). Dynamic crack propagation in elastic-plastic solids. PhD thesis, California Institute of Technology.

Eshelby, J. (1957). The determination of the elastic field of an ellipsoidal inclusion, and related problems. *Proc. R. Soc. Lond.* **A241,** 376–396.

Freund, L. B. (1990). *Dynamic Fracture Mechanics*, Cambridge University Press, Cambridge.

Freund, L. and Douglas, A. (1983). Dynamic growth of an antiplane shear crack in a rate-sensitive elastic-plastic material. *Elastic-Plastic Fracture, Second Symposium, ASTM STP* 803 **1,** 5–20.

Freund, L. and Hutchinson, J. (1985). High strain rate crack growth in rate dependent plastic solids. *J. Mech. Phys. Solids* **33,** 169–191.

Freund, L., Hutchinson, J. and Lam, P. (1986). Analysis of high-strain-rate elastic-plastic crack growth. *Engng Fract. Mech.* **23,** 119–129.

Frost, H. and Ashby, M. (1985). *Deformation Mechanism Maps, The Plasticity and Creep of Metals and Ceramics.* Pergamon Press, Oxford.

Fuller, K. N. G., Fox, P. G. and Field, J. E. (1975). The temperature rise at the tip of fast moving cracks in glassy polymers. *Proc. R. Soc. Lond.* **A.341,** 537–557.

Hui, C. and Riedel, H. (1981). The asymptotic stress and strain field near the tip of a growing crack under creep conditions. *Int. J. Fract.* **17,** 409–425.

Kallivayalil, J. (1995). Thermo-mechanical modelling of crack tip temperature fields. PhD thesis, Cornell University.

Kallivayalil, J. and Zehnder, A. (1994). Measurement of the temperature field induced by dynamic crack growth in beta-c titanium. *Int. J. Fract.* **66,** 99–120.

Krishnakumar, R., Narasimhan, R. and Prabhakar, O. (1989a). Dynamic growth of tensile cracks by ductile and brittle fracture mechanisms in a viscoplastic material. Technical report, *Report ARDB-STR-TR*-89-519-02, IIT Bombay.

Krishnakumar, R., Narasimhan, R. and Prabhakar, O. (1989b). Finite element analysis of dynamic crack growth under plane stress in a viscoplastic material. Technical report, *Report ARDB-STR-TR*-89-519-03, IIT Bombay.

Krishnakumar, R., Narasimhan, R. and Prabhakar, O. (1989c). Temperature rise in a viscoplastic material during dynamic crack growth. Technical report, *Report ARDB-STR-TR*-89-519-01, IIT Bombay.

Kuang, Z. and Atluri, S. (1985). Temperature field due to a moving heat source: A moving mesh finite element analysis. *J. App. Mech.* **52,** 274–280.

Lam, P. and Freund, L. (1985) Analysis of dynamic growth of a tensile crack in an elastic-plastic material. *J. Mech. Phys. Solids* **33,** 153–167.

Rice, J. R. and Levy, N. (1969). Local heating by plastic deformation at a crack tip. In *The Physics of Strength and Plasticity* (Edited by A. Argon), pp. 227–293. MIT Press, Cambridge, MA.

Schwartz, L. (1966). *Mathematics for the Physical Sciences.* Addison Wesley, Reading, MA.

Stroh, A. (1957). A theory of the fracture of metals. *Advances in Physics* **6,** 416–465.

Sung, J. and Achenbach, J. (1987). Temperature at a propagating crack tip in a viscoplastic material. *J. Thermal Stresses* **10,** 243–262.

Vekua, I. N. (1962). *Generalized Analytic Functions.* Addison Wesley, Reading, MA.

Weichert, R. and Schonert, K. (1974). On the temperature rise at the tip of a fast running crack. *J. Mech. Phys. Solids* **22,** 127–133.

Wilson, D. and Esler, C. (1983). Properties of ti-3al-8v-6cr-4mo-4zr. In *Beta Titanium Alloys in the* 1980's, pp. 457–482, Metallurgical Society of AIME, Warrendale, PA.

Wu, K. C. (1985). Analysis of steady state crack propagation in ductile materials. PhD thesis, Cornell University.

Wu, K. C. and Hui, C. Y. (1987). A complex-variable method for two-dimensional internal stress problems and its applications to crack growth in nonelastic materials: Part 1-theory. *J. App. Mech.* **54,** 59–64.

Wu, K. C. (1988). Stress intensity factors due to non-elastic strains and body forces for steady dynamic crack extension in an anisotropic elastic material. *Int. J. Solids Structures* **24,** 805–815.

Yang, W. and Freund L. B. (1986). An analysis of anti-plane shear crack growth in a rate sensitive elastic-plastic material. *Int. J. Fract.* **30** 157–174.